International Journal of Computational and Theoretical Chemistry
2020; 8(2): 27-39
http://www.sciencepublishinggroup.com/j/ijctc
doi: 10.11648/j.ijctc.20200802.11
ISSN: 2376-7286 (Print); ISSN: 2376-7308 (Online)

Effect of Substituents on Electronic Structure and Photophysical Properties of Re(I)$(CO)_3$Cl(R-2, 2'-Bipyridine) Complex: DFT/TDDFT Study

Dereje Fedasa[1, *], Dunkana Negussa[2], Alemu Talema[1]

[1]Department of Chemistry, College of Natural and Computational Sciences, Injibara University, Injibara, Ethiopia

[2]Department of Chemistry, College of Natural and Computational Sciences, Wollega University, Nekemte, Ethiopia

Email address:

fedasadereje2009@gmail.com (D. Fedasa)

[*]Corresponding author

To cite this article:

Dereje Fedasa, Dunkana Negussa, Alemu Talema. Effect of Substituents on Electronic Structure and Photophysical Properties of Re(I)$(CO)_3$Cl(R-2, 2'-Bipyridine) Complex: DFT/TDDFT Study. *International Journal of Computational and Theoretical Chemistry*. Vol. 8, No. 2, 2020, pp. 27-39. doi: 10.11648/j.ijctc.20200802.11

Received: March 5, 2020; **Accepted**: March 24, 2020; **Published**: November 11, 2020

Abstract: The electronic structure, absorption and emission spectra, as well as phosphorescence efficiency of Re(I) tricarbonyl complexes of a general formula *fac*-[Re(I)$(CO)_3$(L)(R-N^N)](L = Cl; N^N = 2, 2'-bipyridine; R = -H, 1; -NO_2, 2; -$PhNO_2$, 3; -NH_2, 4; -TPA (triphenylamine), 5) were investigated by using density functional theory(DFT) and time dependents density functional theory (TDDFT) methods. The calculated results reveal that introductions of the Electron with drawing group (EWG) and Electron donating group (EDG) on the R position of 2, 2'-bipyridine ligand. When EWG (-NO_2 and -$PhNO_2$) are introduced into complex 2 and 3, the lowest energy absorption and emission bands are red shifted compared with that of complex 1. On the contrary, the introduction of the EDG (-NH_2 and -TPA) in complex 4 and 5 cause corresponding blue shifted. The solvent effect on absorption and emission spectrum indicates that the lowest energy absorption and emission bands have red shifts with the decrease of solvent polarity. The electronic affinity (EA), ionization potential (IP) and reorganization energy (λ) results show that complex 5 is suitable to be used as an emitter in phosphorescence organic light emitting diodes (PHOLEDs). Meanwhile the emission quantum yield of complex 5 is possibly higher than that of other complexes.

Keywords: Electronic Structure, Internal Quantum Efficiency, Luminescence, Phosphorescence and Photophysical Properties

1. Introduction

Organic light emitting diodes (OLEDs) are solid state electronic devices which emit light in response to the applied electric current. Among different types of OLEDs, PHOLEDs are the classes of OLED that use the principle of phosphorescence to offer four times the internal efficiency of conventional fluorescent OLEDs. Light emitting organic materials has phosphorescent materials which serve as recombination centers for electrons and holes to produce the electronic excited states are mainly captivating. Because, they harvest light from both singlet and triplet excitons and enabling the devices with close to 100% internal quantum efficiency [1]. However, exploration of novel materials including emitting materials and host materials is crucial to push the performance of the PHOLEDs [2]. PHOLEDs have attracted worldwide attention over the past decades due to their unique features and huge potential for flat panel, flexible display, energy saving solid state lighting and virtual reality [3].

The highly efficient PHOLEDs can be designed from the 3^{rd} row d^6 transition metal complexes with appropriate organic ligand because, existence of transition metal in complex exhibit strong spin orbit coupling (SOC) which substantially accelerates singlet to triplet intersystem crossing ISC [4-6]. Selection of organic ligand allows different electronic transitions occurring between different energy states associated with metal atom is important to design highly efficient luminescent complexes [7-9]. The specific photophysical properties of bidentate hetero-aromatic

diamine ligand complexes with third row d^6 transition metal ions such as Re(I), Ru(II) and Os(II) are significant. Among them Re(I) tricarbonyl complexes with substituted 2, 2'-bipyridine ligand attached rhenium often show intense and long lived luminescence. 2, 2'-bipyridine is a bidentate ligand with powerful binding abilities towards Re(I) metal ion. It can be easily modified by the introduction of different substituent groups at its different positions. Introduction of electron with drawing group (EWG) or electron withdrawing group (EDG) substituent is useful to tune the energy level of 2, 2'-bipyridine ligand to provide high efficiency PHOLED [10-15].

On the other hand, in the PHOLED system, unbalanced charge transport for electrons and holes in the emission layer results in low luminescence efficiency and less internal quantum efficiency. Because, these complexes are fairly good electron transport materials while hole transport ability is poorer [16]. The authors has tried to solve the problem of the internal quantum efficiency and low luminescence efficiency of this complex in the PHOLED system by tuning electronic structure and photophysical properties of Re(I) tricarbonyl complexes with varying substituent on the 2, 2'-bipyridine ligand theoretically through DFT and TDDFT study. To overcome less internal quantum efficiency and low luminescence efficiency PHOLEDs problem, incorporation of hole transporting groups to the 2, 2'-bipyridine ligand of Re(I) tricarbonyl complex can be an alternative option. The structures of *fac*-[Re(I)$(CO)_3$L(R-N^N)] where, (L = Cl, N^N = 2, 2'-bipyridine, R = -H, 1; -NO_2, 2; -$PhNO_2$, 3; -NH_2, 4; -TPA, 5 under the study shown as below:

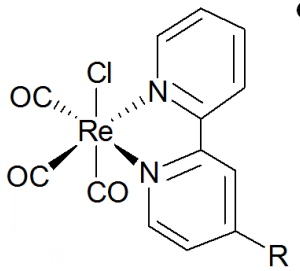

Complex	R
1	-H
2	-NO_2
3	-$PhNO_2$
4	-NH_2
5	-TPA

Figure 1. *The structures of Re(I) tricarbonyl complexes having a general formula fac-[Re(I)$(CO)_3$Cl(R-2, 2'-bipyridine)] with replacement of its substituted groups.*

2. Computational Methodology

The singlet ground state (S_0) and lowest lying triplet excited state (T_1) geometries of all complexes were optimized using the DFT method in the gas phase [2]. The B3LYP exchange correlation functional provides enough accurate information on the ground and excited state properties of the complex [17-18]. A double-ζ quality LANL2DZ basis set is applied for Re atom together with 6-311++G(d, p) basis set for C, H, N, O and Cl atoms. Both LANL2DZ for Re and 6-311++G(d, p) for other atoms basis set are also written in the additional input under Gaussian calculation set up [19-23]. Vibrational frequency analyses were performed to confirm that the optimized structures were true minimum or stable structures. Vibrational frequency calculations in which there is an absence of imaginary frequency for all configurations, confirm that they are minimum point on the potential energy surface. HOMO and LUMO contour plot and energy level of all complexes were obtained from optimized structures.

Excited state calculations were studied using the TDDFT method on the basis of an optimized structure of all the complexes with the same functional and basis sets [24-25]. On the basis of optimized S_0 and T_1 structures, TDDFT method was used to calculate the electronic absorption and phosphorescence spectra of the complexes, respectively. Absorption spectra of 1 - 5 complexes were simulated in the GAMESS software to obtain best spectra. In order to incorporate the effect of the solvent around the molecule, the polarizable continuum model (PCM) is used in the TDDFT calculation [5]. The calculated electronic density plots for the FMOs were performed by Gauss View 5.0.8 software. In addition, the positive and negative ions with regard to "electron - hole" creation are relevant to their use as OLED materials. Thus, the ionization potentials (IP), electron affinities (EA) and reorganization energies (λ) were obtained by comparing the energy levels of the neutral molecule with the positive ions and negative ions, respectively. All calculations were performed using Gaussian 09 software package [26].

3. Results and Discussion

3.1. The Optimized Geometries in the Ground States and Lowest Triplet States

The structures of the studied Re(I) tricarbonyl with substituted R positions of 2, 2'-bipyridine ligand by -H, -NO_2, -$PhNO_2$, -NH_2 and -TPA complexes are shown in Figure 1. Optimized ground state geometries of 1 - 5 complexes are shown in Figure 2. The selected bond lengths and bond angles of 1 - 5 complexes in the optimized ground state (S_0) and the lowest lying triplet state (T_1), as well as the experimental values of complex 1 based on crystallographic data taken from the literature [34] are collected in Table 1. The geometry consists of the 2, 2'-bipyridine ligand, three carbonyl ligands and chlorine atom around the Rhenium atom. The stability of optimized geometries of all complexes was confirmed by frequency calculations in which there is no imaginary frequency for all configurations. It can be seen from Figures 1 and 2 that Re(I) tricarbonyl with substituted R position of 2, 2'-bipyridine ligand complexes have an analogous octahedral coordination around the Re atom with Cl atom, 2, 2'-bipyridine and three CO ligands in a facial configuration. Table 1 shows that the bond lengths and bond angles in 1-5 complexes display typical features of Re(I) tricarbonyl diamine complexes.

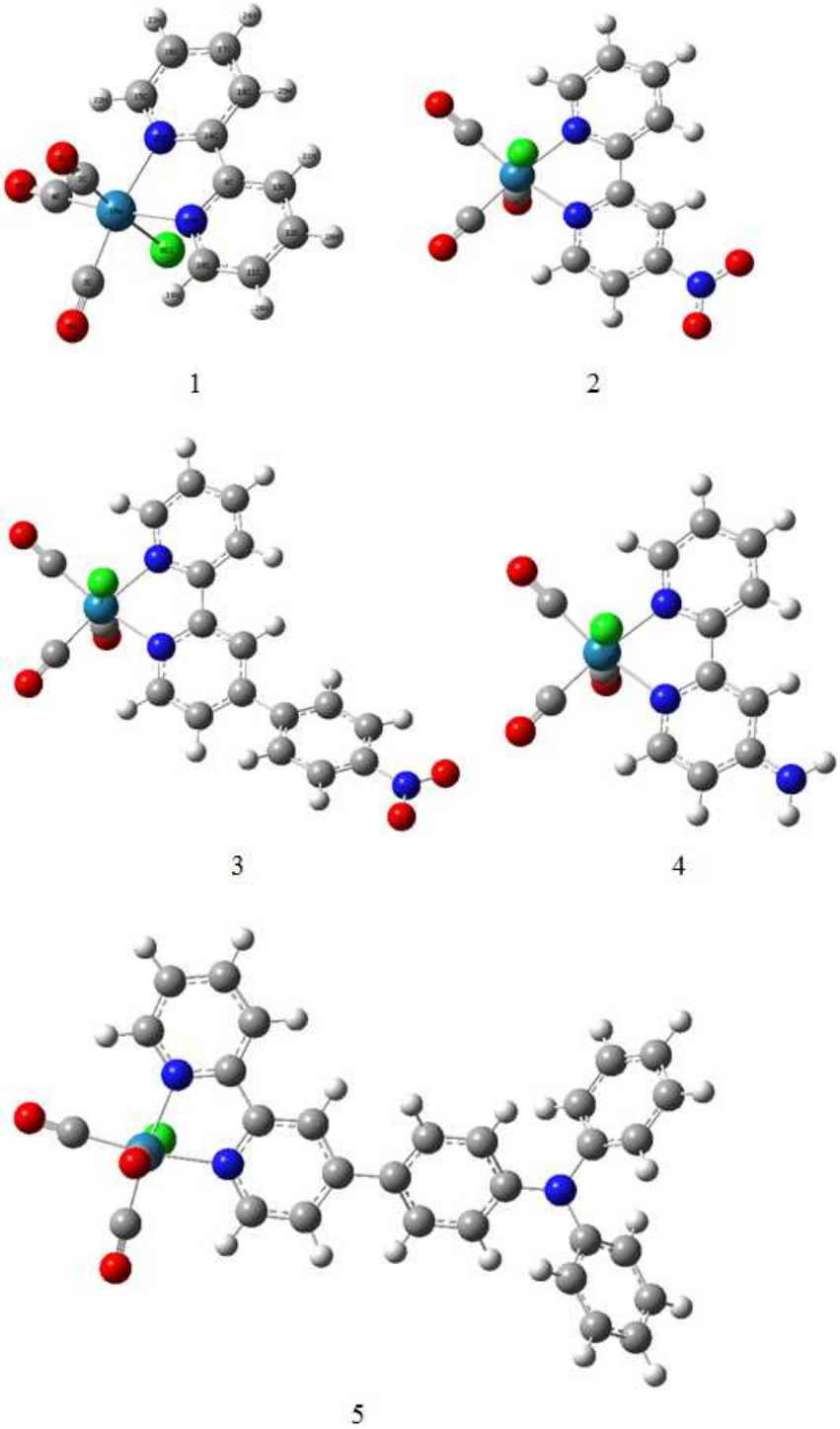

Figure 2. *The optimized geometries of fac-[Re(I)(CO)$_3$Cl(R-2, 2'-bipyridine)] where, R = -H, 1; -NO$_2$, 2; -PhNO$_2$, 3; -NH$_2$, 4 and -TPA, 5 determined at B3LYP/6-311++G(d, p)/LANL2DZ level in the ground state.*

The optimized parameters of complex 1 are in good agreement with the experimental values based upon crystallographic data taken from literature [34]. It gives positive indication on the reliability of the theoretical method. The slight deviations between calculated and experimental values are due to the fact that the effects of crystal packing and chemical environment. The effects of both crystal packing and chemical environment are not considered in theoretical calculations. Theoretical calculations refer to gas phase but experimental results are from the close packed crystal lattice. The substitution of the R position of 2, 2'-bipyridine ligand by different EWG and EDG give rise to negligible changes for the bond lengths and bond angles in 1 - 5 complexes in S_0 state as it is shown in Table 1. There is a typical angle about 90^0 among three CO ligands in the *fac*-$Re(CO)_3^+$ unit for all studied complexes. And the axial Re-C bond distance is shorter than the equatorial Re-C bond distances in each complex.

This is attributed to different ligand to metal back bonding ability which is that the axial CO opposite to Cl atom. Therefore, the introduction of R = -H, 1; -NO_2, 2; -$PhNO_2$, 3; -NH_2, 4 and -TPA, 5 groups on the R position of 2, 2'-bipyridine ligand takes a minor effect on their geometric structures in S_0 state.

The calculated geometrical parameters of 1 - 5 complexes in the triplet state (T_1) are also given in Table 1. It also reveals that the introduction of different substituent groups on the R position of 2, 2'-bipyridine ligand gives rise to a little effect on their geometric structures in T_1 state. However, the bond lengths and bond angles of 1 - 5 complexes in T_1 state have obvious changes compared with those in S_0 state. Specifically, the bond lengths of Re-N, Re-Cl are contracted while the bond lengths of Re-C was relaxed. This shows that the interaction between Re(I) and 2, 2'-bipyridine ligand is strengthened, while the interactions between Re(I) and three CO ligands are weakened in T_1 state. Therefore, 2, 2'-bipyridine ligand have a greater effect on FMOs of these complexes in T_1 state. The different strengths between Re(I) and 2, 2'-bipyridine ligand or CO ligands will lead to different electron transition characters.

Table 1. *The selected bond lengths and bond angles of 1 - 5 complexes in S_0 state and T_1 state calculated at the B3LYP/6-311++G(d, p)/LANL2DZ level. Distances are in angstrom and angles are in degree.*

	1(-H)			**2(-NO_2)**		**3(-$PhNO_2$)**	
	Exptl.	**S_0**	**T_1**	**S_0**	**T_1**	**S_0**	**T_1**
Bond Length (Å)							
Re-Cl8	2.574	2.548	2.480	2.543	2.469	2.547	2.483
Re-C2	1.915	1.910	1.952	1.914	1.955	1.911	1.949
Re-C3	1.907	1.925	1.947	1.927	1.942	1.926	1.939
Re-C4	2.058	1.925	1.981	1.931	1.984	1.927	1.985
Re-N26	2.163	2.171	2.137	2.153	2.094	2.170	2.083
Re-N27	2.171	2.171	2.095	2.169	2.159	2.164	2.157
Bond Angles (°)							
N26-Re-N27	74.7	75.48	77.78	75.76	77.27	75.41	77.24
C2-Re-C4	95.9	91.82	89.45	91.69	88.67	91.79	88.77
C2-Re-C3	90.3	91.82	93.92	91.68	92.96	91.79	92.49
C2-Re-N26	90.7	93.83	90.72	94.26	92.61	94.00	93.22
C2-Re-N27	86	93.83	90.13	94.08	89.74	93.72	90.45
C3-Re-N27	97.5	97.01	96.66	96.79	96.71	97.02	96.44
C4-Re-N26	97.8	97.01	98.03	96.85	97.55	97.06	96.99
C4-Re-Cl8	-	91.24	86.77	91.12	90.47	91.08	90.16

	4(-NH_2)		**5(-TPA)**	
	S_0	**T_1**	**S_0**	**T_1**
Bond Lengths (Å)				
Re-Cl8	2.551	2.499	2.551	2.513
Re-C2	1.907	1.942	1.909	1.933
Re-C3	1.923	1.982	1.924	1.934
Re-C4	1.923	1.939	1.925	1.970
Re-N26	2.171	2.079	2.172	2.156
Re-N27	2.173	2.143	2.167	2.086
Bond Angles (°)				
N26-Re-N27	75.23	77.73	75.32	77.27
C2-Re-C4	91.83	92.15	91.79	89.91
C2-Re-C3	91.83	89.02	91.79	92.21
C2-Re-N26	93.52	90.58	93.88	93.27
C2-Re-N27	93.80	93.59	93.60	91.45
C3-Re-N27	97.13	96.02	97.03	96.23
C4-Re-N26	97.17	96.14	97.15	96.61
C4-Re-Cl8	91.34	89.52	90.99	89.91

Experimental values from [34]. Calculated optimized parameters shows octahedral coordination structure and interaction between Re (I) and 2, 2'-bipyridine ligand of all complexes.

3.2. Molecular Orbital Properties

The properties of the frontal molecular orbital (FMOs) have a significant effect on the excited states and electronic transitions of OLED materials. It is well known that the optical properties of the complexes are associated with FMOs especially, HOMO and LUMO [27].

The contour plots of HOMO (H) and LUMO (L) of 1 - 5 complexes are shown in Figure 3 and the main FMO energy levels are plotted in Figure 4.

It can be seen that HOMOs of 1 - 5 complexes mainly consist d orbitals of Rhenium atom [d(Re)], p orbitals of chlorine atom [p(Cl)] and π orbitals of three CO ligands [π(CO)] while LUMOs predominantly contributed from π* anti-bonding orbitals of 2, 2'-bipyridine ligand with its substituents. The introductions of different substituent groups on 2, 2'-bipyridine ligand have little effect on FMOs compositions. According to Figure 4, when EWG and EDG groups were introduced on the R position, the energy levels of HOMOs changes little. But energy levels of LUMOs shows significant variation due to different substituent groups attached on the 2, 2'-bipyridine ligand. The introductions of EWGs (R = $-NO_2$, 2 and $-PhNO_2$, 3) decreases the energy level of LUMO (E_{LUMO}) while the introductions of EDGs (R = $-NH_2$, 4 and -TPA, 5) increases E_{LUMO}. The order is E_{LUMO} (-2.816 eV) (4) > E_{LUMO} (-2.904 eV) (5) > E_{LUMO} (-3.122 eV) (1) > E_{LUMO} (-3.8974 eV) (3) > E_{LUMO} (-4.447 eV) (2). Therefore, the energy gap of 1 - 5 complexes decreases with the electron withdrawing substituent group and increases with electron donating substituent groups.

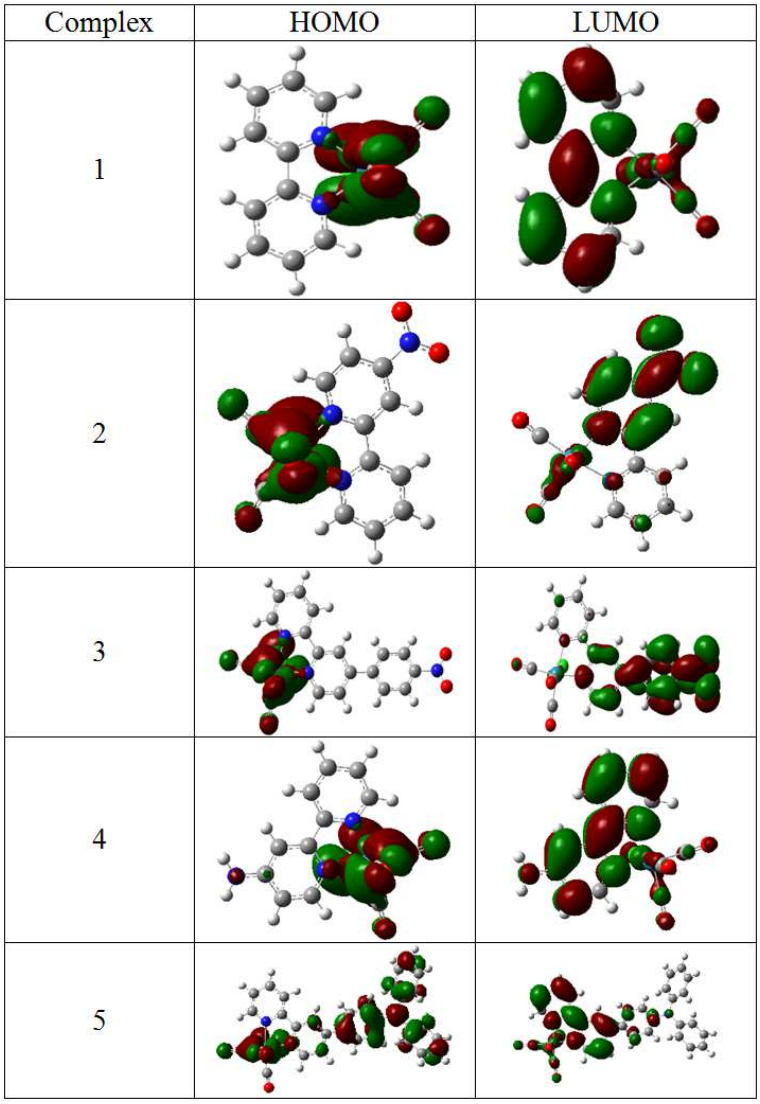

Figure 3. *Contour plot of HOMO and LUMO of 1 - 5 complexes.*

3.3. Absorption Spectra

Based on the optimized ground state geometry, the absorption properties of 1 - 5 complexes have been determined. TDDFT/B3LYP/LANL2DZ (for Re atom) and 6-311++G(d, p) (for C, H, N, O and Cl atoms) theoretical method with PCM in CH_2Cl_2 media was used to calculate absorption spectra of all complexes. The transition behavior, the relevant energies/wavelengths, oscillator strength, dominant orbital excitations with configuration interaction (CI) coefficients and their assignments as well as experimental values from the literature [34] of complex 1 are collected in Table 2. By using GAMESS software, the corresponding simulated UV-Visible absorption spectra of 1 - 5 complexes are sketched in Figure 5. For complex 1, the calculated lowest lying energy absorption is at 423 nm, which is assigned to electronic transition from H-1 to L. HOMO is contributed by [d(Re) + p(Cl) + π(CO)], while

LUMO predominantly located on π*(2, 2'-bipyridine). H-1 and L+1 have a similar charge transfer character with H and L. The MLCT type is commonly observed in the lowest energy transitions for transition metal complex [28-29].

So this electronic transition can be described as [d(Re) + p(Cl) + π(CO)] → π* (2, 2'-bipyridine) with MLCT/XLCT/LLCT is in good agreement with the experimental value 420 nm. The moderately intense band is at 448 nm. Similarly, the transition of this band is from H to L with characteristic MLCT/XLCT/LLCT. The strong absorption at 316 nm is from H to L+2 with LLCT/XLCT character. Therefore, it indicates that the calculated value is precise and reliable to explain absorption spectra. As observed in table 2, the lowest energy and moderately intense absorption bands of complexes 2 - 5 have a similar transition character as compared to the absorption bands of complex 1. But the strong absorption bands of complexes 2 and 3 are different from that of complex 1. Specifically, for complex 2, the strongest absorption band at 420 nm is from H-3 to L with LLCT/XLCT character. For complex 3, the strong absorption band at 419 nm is also from H-1 to L+1 with MLCT/LLCT/XLCT character. Moreover, for complexes 4 and 5, the strong absorption bands are different from bands of complex 1.

For complex 4, the transition character of a strong absorption band is H-3 to L which is having a mixed character of XLCT/ILCT while the absorption band of complex 5 is assigned to H-3 to L and H to L+2 excitations with mixing MLCT/XLCT/LLCT. From Figure 5, it can intuitively be seen that the calculated absorption bands for 1 - 5 complexes have almost identical profiles but the positions of absorption bands are different. It is noteworthy that the contribution of MLCT is more remarkable in the lowest energy absorption bands with the large compositions of Re atom in HOMOs and HOMO-1s. The lower energy absorption bands of 1 - 5 complexes follow the order: 2 (634nm) > 3 (505nm) > 1 (423nm) > 4 (404nm) > 5 (400nm). It reveals that the introduction of EWG on 2, 2'-bipyridine ligand (mainly for complex 2 and 3) absorption bands red shifted (longer wavelength). On the hand when EDG substituents introduced on 2, 2'-bipyridine ligand (complex 4 and 5) the absorption band become the blue shifted (shorter wavelength).

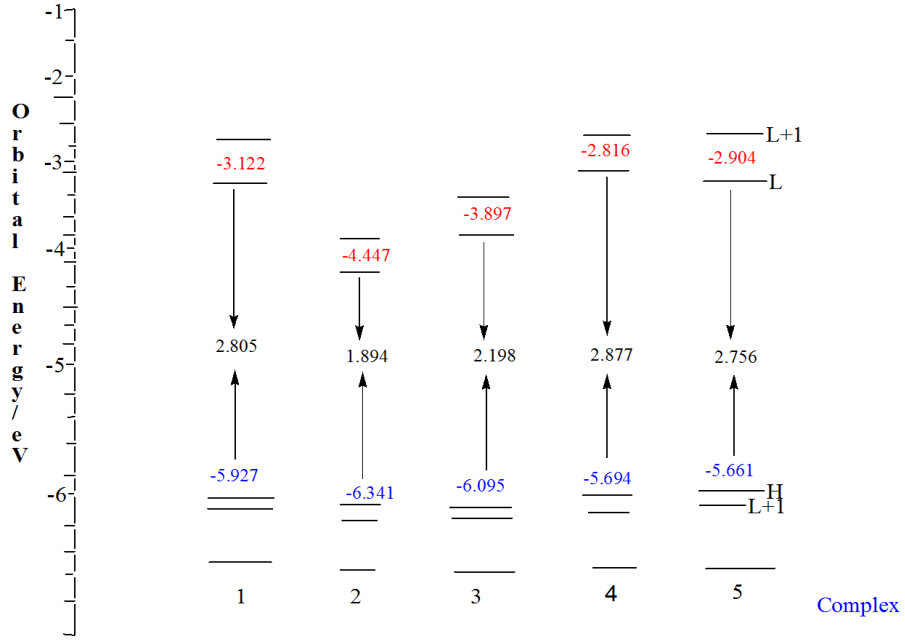

Figure 4. *The main FMO energy level of 1 - 5 complexes.*

Table 2. *The calculated energies/wavelengths, oscillator strengths, transition character, dominant orbital excitations with CI and their assignments for all complexes calculated at TDDFT/B3LYP/LANL2DZ(for Re atom)/6-311++G(d, p)(for C, H, N, O, Cl) level in CH_2Cl_2 media and experimental values of complex 1 from the literature.*

	E(eV/nm)	Oscillator strength	Transition	|CI|	Assign	λ_{exp}(nm)
1	2.765/448	0.0027	H→L	0.704	MLCT/XLCT/LLCT	420nm
	2.929/423	0.0680	H-1→L	0.703	MLCT/XLCT/LLCT	
	3.275/378	0.0002	H-2→L	0.702	MLCT/XLCT/LLCT	
	3.804/325	0.0005	H→L+1	0.686	MLCT/XLCT/LLCT	
	3.906/317	0.0004	H-1→L+1	0.580	MLCT/XLCT/LLCT	
	3.919/316	0.0047	H →L+2	0.490	LLCT/XLCT	
2	1.761/703	0.0039	H→L	0.6852	MLCT/XLCT/LLCT	-
	1.953/634	0.0852	H-1→L	0.6865	MLCT/LLCT/LLCT	
	2.314/535	0.0002	H-2→L	0.7003	MLCT/XLCT/LLCT	
	2.829/438	0.0039	H→L+1	0.6951	MLCT/XLCT/LLCT	
	2.944/421	0.0076	H-1→L+1	0.5815	MLCT/XLCT/LLCT	
	2.950/420	0.0058		0.6137	LLCT/XLCT	

	E(eV/nm)	Oscillator strength	Transition	|CI|	Assign	λ_{exp}(nm)
3	2.345/529	0.0179	H→L	0.673	MLCT/XLCT/LLCT	-
	2.454/505	0.0843	H-1→L	0.687	MLCT/XLCT/LLCT	
	2.822/439	0.0015	H→L+1	0.676	MLCT/XLCT/LLCT	
	2.888/429	0.0001	H-2→L	0.667	MLCT/XLCT/LLCT	
	2.958/419	0.0455	H-1→L+1	0.687	MLCT/XLCT/LLCT	
	3.261/380	0.0025	H-9→L	0.677	LLCT/XLCT	
4	2.896/428	0.0111	H→L	0.6775	MLCT/XLCT/LLCT	-
	3.063/404	0.0781	H-1→L	0.6785	MLCT/XLCT/LLCT	
	3.439/360	0.0002	H-2→L	0.6966	MLCT/XLCT/LLCT	
	3.689/336	0.0382	H-3→L	0.6831	XLCT/LLCT	
	3.769/328	0.0027	H→L+1	0.6952	MLCT/XLCT/LLCT	
	3.901/317	0.0111	H-1→L+1	0.6857	MLCT/XLCT/LLCT	
5	2.348/528	0.3559	H→L	0.703	MLCT/XLCT/LLCT	-
	2.793/443	0.0017	H-1→L	0.699	MLCT/XLCT/LLCT	
	2.948/420	0.0804	H-2→L	0.695	MLCT/XLCT/LLCT	
	3.096/400	0.5118	H→L+1	0.699	MLCT/XLCT/LLCT	
	3.297/376	0.0000	H-3→L	0.701	XLCT/LLCT	
	3.381/366	0.0401	H→L+2	0.701	XLCT/LLCT	

Experimental values from [34]

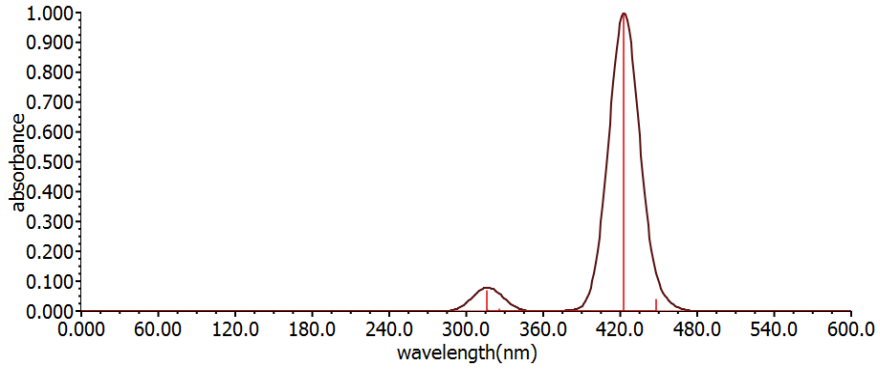

1

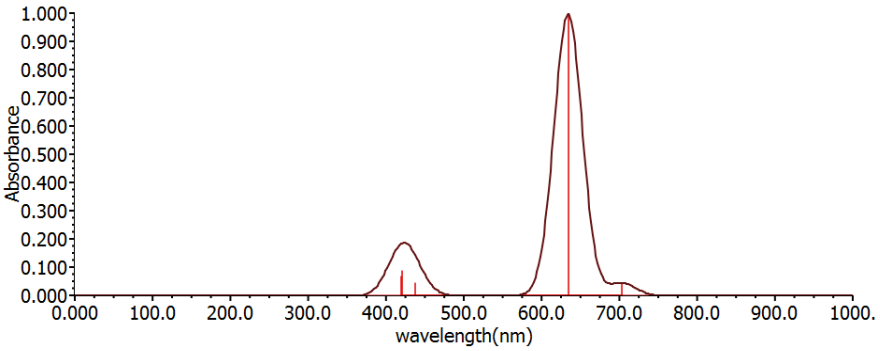

2

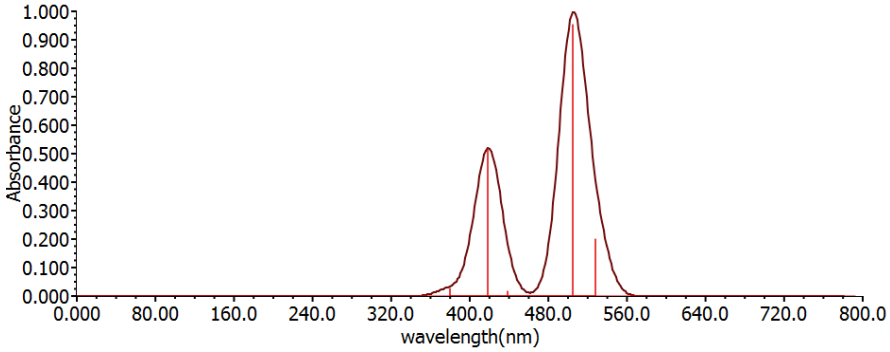

3

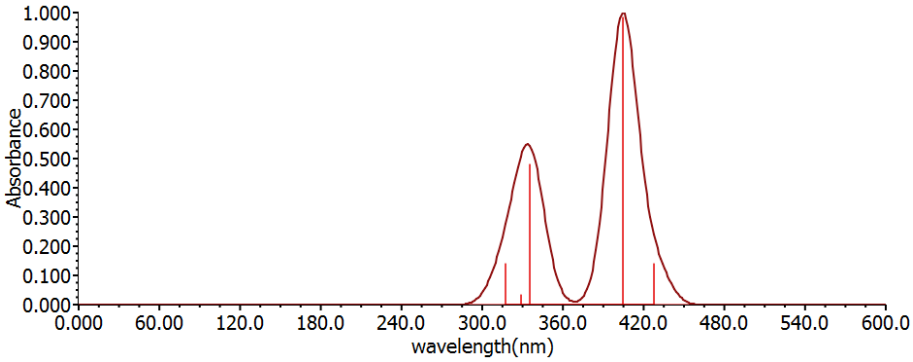

4

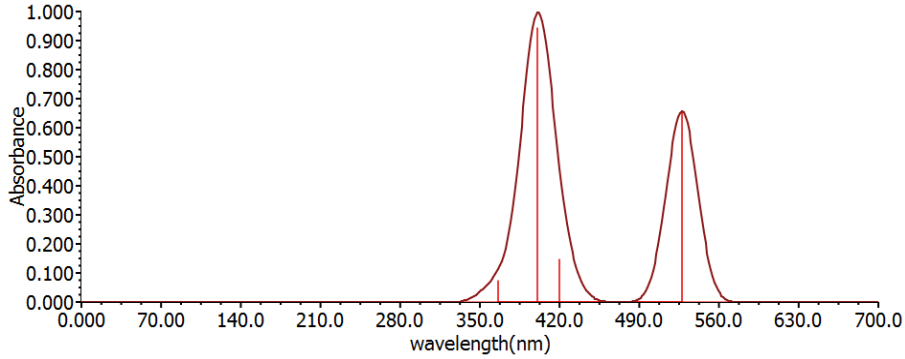

5

Figure 5. *The simulated UV-Vis absorption spectra of 1 - 5 complexes.*

The contribution of MLCT/XLCT/LLCT is remarkable in lowest energy absorption band with the order of 2 > 3 > 1 > 4 > 5. All spectra have identical profiles but they have different absorption bands.

3.4. Phosphorescence Spectra

With the optimized T_1 structures as the starting point, the emission spectra of complexes 1 - 5 were determined by the TDDFT/B3LYP methods with PCM in CH_2Cl_2 media. The energy/wavelengths, dominant transitions with larger CI coefficients and their assignments are collected in Table 3. The contour plots of HOMO and LUMO for all complexes are shown in Figure 6 and main FMOs energy levels are plotted in Figure 7. Table 3 shows that the energy emissions of 1 - 5 complexes mainly originate from LUMO to HOMO transition. According to Table 3, it also can be seen that LUMOs are mainly localized on π*(2, 2'-bipyridine) orbital for all complexes, while HOMOs are primarily on [d(Re)], [p(Cl)] and π(CO) ligands. To intuitively understand the emission transition, the plots of HOMO and LUMO emissions of 1 - 5 complexes are presented in Figure 6.

For 1 - 5 complexes, HOMO energy levels are similar to each other, but LUMO energy levels present an obvious variation. The introduction of -NO_2 and $PhNO_2$ on R position of 2, 2'-bipyridine ligand can decrease the E_{LUMO}. The introduction of -NH_2 and -TPA increases the E_{LUMO}. So, the introductions of -NO_2 and -$PhNO_2$ lead to the lowest energy emission bands red shifted relative to complex 1. The introduction of -NH_2 group in complex 4 and -TPA in complex 5 can cause a corresponding blue shift. Moreover, complex 5 emit light in the visible range, but other complexes occur in the near-infrared region. There is no experimental assignment for the emissions of these complexes [30]. Therefore, the introduction of stronger electron donating group on the R positions of 2, 2'-bipyridine ligand blue-shifted the spectra with the lowest energy emission band.

Table 3. *The calculated energies/wavelengths, the dominant orbital excitations with large configuration interaction (CI) and assignments of 1 - 5 complexes.*

Complex	E (eV/nm)	Transition	|CI|	Assignment
1	1.3603/911	L→H	0.9313	^{3}MLCT/^{3}XLCT/^{3}LLCT
2	1.142/1085	L→H-1	0.9718	^{3}MLCT/^{3}XLCT/^{3}LLCT
3	0.836/1483	L→H	0.8304	^{3}MLCT/^{3}XLCT/^{3}LLCT
4	1.4271/869	L→H	0.8832	^{3}MLCT/^{3}XLCT/^{3}LLCT
5	1.5815/784	L+3→H	0.6790	^{3}MLCT/^{3}XLCT/^{3}LLCT

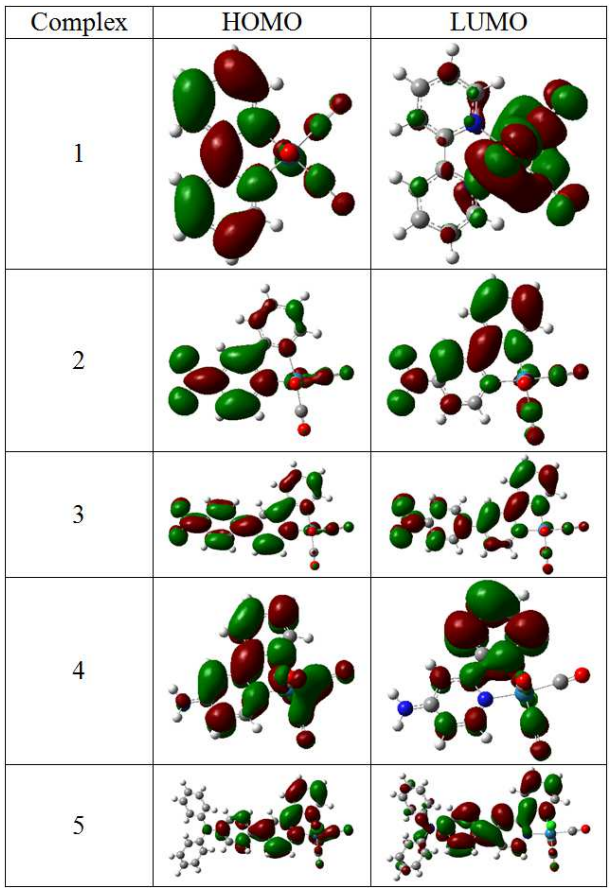

Figure 6. *The contour plots of excited state HOMO and LUMO of 1 - 5 complexes.*

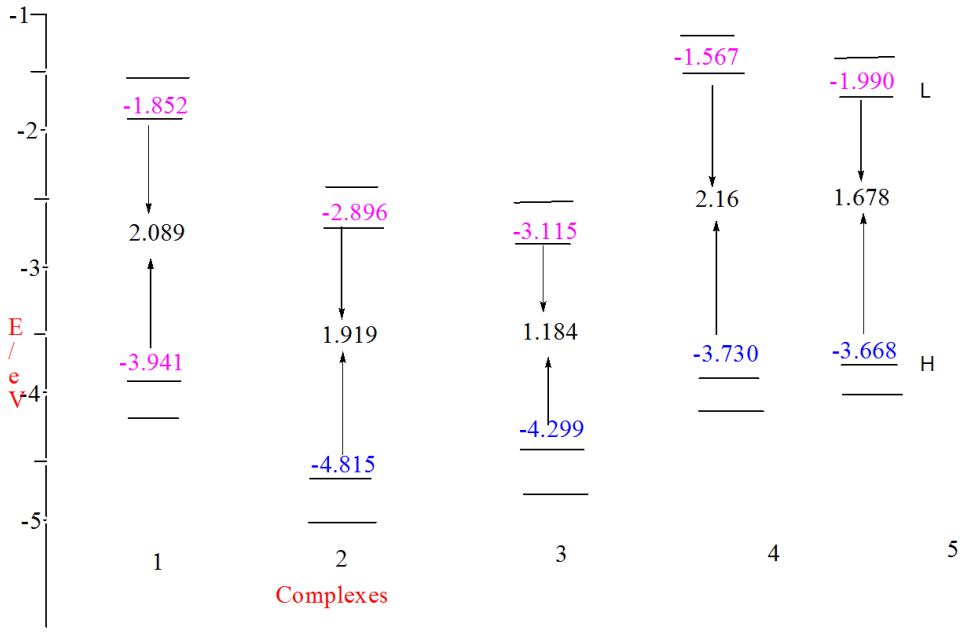

Figure 7. *The main FMOs energy levels of the 1 - 5 complexes in the excited state.*

3.5. Effect of Solvent on Absorption and Emission Spectra

Different solvents have different polarity. Different solvents can cause different excitation energies due to their polarity. For the lowest energy absorption and emission wavelengths, solvent effects are assessed using the PCM method as shown in Table 4 for complexes 1 - 5. Both the lowest energy absorption and emission bands have red shifted (longer wavelength) with the decrease in solvent polarity while blue shifted (shorter wavelength) with the increase in solvent polarity for all complexes. Compared with the experimental

method, it is easy for theoretical calculations to change solvents. This is another advantage of theoretical calculations.

Table 4. *The lowest energy absorption and emission wavelength of 1 - 5 complexes in the different polarity solvents in case of dichloromethane, acetone and methanol.*

Solvent	Polarity	Absorption (nm)					Emission (nm)				
		Complex					Complex				
		1	2	3	4	5	1	2	3	4	5
CH_2Cl_2	3.4	423	634	505	404	400	935	935	939.5	841	1195
CH_3COCH_3	5.4	412	617	493	395	399	842	914	939	837	1193
CH_3OH	6.6	409	612	489	391	398	840	906	938	835	1189

3.6. Electronic Affinity (EA), Ionization Potential (IP) and Reorganization Energy (λ)

The electronic affinity (EA), ionization potential (IP) and reorganization energy (λ) are very significant in performance ability of PHOLED materials. IP and EA are usually used to assess the energy barrier for the injection of holes and electrons from the anode into the emitting materials [31]. The EA can be either for vertical excitations or adiabatic excitations denoted by EA (v) and EA (a). Similarly, IP is denoted by IP (v) and IP (a). The IP_V is defined as the energy difference between the cation and its neutral molecule at the equilibrium geometry of the neutral molecule. The IP_a is defined as the energy difference between the cation and its neutral molecule at their own equilibrium geometries. The E_{Av} is defined as the energy released when the electron is added to the neutral molecule computed as the energy difference between the neutral form and the anion. The EA_a is defined as the energy difference between the neutral molecule and its anion at their own equilibrium geometries. The HEP is the energy difference between neutral molecules and cationic systems calculated using a cationic geometric structure. Similarly, the EEP is the energy difference between neutral molecules and anionic systems calculated using anionic geometric structures. In this study vertical and adiabatic of EA and IP (EAv, EAa, IPv, and IPa), EEP, HEP, electron transport reorganization energy ($\lambda_{electron}$), hole transport reorganization energy (λ_{hole}) and the difference between λ_{hole} and $\lambda_{electron}$ for all complexes were calculated with DFT method and collected in Table 5. The introduction of EWG on R position facilitates the electron injection ability, while the introduction of EDG facilitates the hole injection ability. As shown in Table 5, it can be found that all of the complexes possess lower $\lambda_{electron}$ in comparison to λ_{hole} except complex 5, which reveal that electron transporting performance is slightly better than hole transporting performance. This means that all of these complexes can be used as electron transporting materials. But, as it can be seen complex 5 has a relatively small difference between $\lambda_{electron}$ and λ_{hole} which can improve the charge transfer balance and further enhance the device performance of PHOLEDs. So complex 5 is more suitable to be used as an emitter in OLEDs in this regard. The above analysis result reveals that the different substituent groups on the R position of 2, 2'-bipyridine ligand can influence charge transfer rates of electrons and holes. In this case, we hope that theoretical investigations can guide experiment to develop novel and efficient materials of OLEDs.

Table 5. *The calculated vertical and adiabatic of EA and IP (EAv, EAa, IPv and IPa all in eV), EEP in eV, HEP in eV, $\lambda_{electron}$ in eV, λ_{hole} in eV and the difference between λ_{hole} and $\lambda_{electron}$ of the complexes.*

Complex	EA_V	EA_a	IP_V	IP_a	HEP	EEP	λ_e	λ_h	λ_{h-e}
1	-1.954	-1.785	7.622	7.416	7.195	-1.619	0.335	0.425	0.092
2	-3.185	-3	7.969	7.769	7.55	-2.813	0.372	0.419	0.047
3	-2.857	-7.396	2.987	2.781	7.271	-7.222	-4.365	-4.284	0.081
4	-1.721	-1.525	7.344	7.101	6.827	-1.325	0.396	0.517	0.121
5	-2.029	-1.839	6.713	6.645	6.566	-1.652	0.377	0.147	-0.23

3.7. The Emission Quantum Yield in CH_2Cl_2 Media

The emission quantum yield (Φ) can be affected by the competition between radiative decay rate constant (K_r) and non-radiative decay rate constant (K_{nr}) [32].

$$\Phi = K_r \tau_{em} = \frac{k_r}{k_r + k_{nr}} \quad (1)$$

Where, τ_{em} is the emission decay time. From the above formula, the large K_r and small K_{nr} are required to increase the value of emission quantum yield (Φ). The K_r and K_{nr} can expressed as:

$$K_r \approx \left(\frac{\langle \Psi_{S1} | H_{S0} | \Psi_{T1} \rangle^2 \mu^2_{S1}}{(\Delta E_{S1\text{-}T1})^2} \right) \quad (2)$$

$$= \frac{(16\pi^3 10^6 n^3 E_{T1}{}^3)}{3h\varepsilon_0} \quad (3)$$

$$K_{nr} = \alpha e^{(-\beta E_{T1})} \quad (4)$$

Where, α and β are constant, μ_{S1} is transition electric dipole moment from S_0 to S_1. $\Delta E_{S1\text{-}T1}$ is the energy gap between S_1 and T_1 states, E_{T1} is the energy of the lowest triplet excited state for phosphorescence and n, h and ε_0 are refractive index,

plank's constant and permittivity in a vacuum, respectively. Therefore, the variation of Φ can be qualitatively calculated from the above formulas. According to above equation when E_{T1} value increase, K_r may increase and K_{nr} may decrease. The corresponding data are summarized in Table 6. It can be seen from the table that complex 5 has the largest E_{T1} (1.581 eV), which may increase the value of Φ. The SOC effects can be elucidated mainly from the energy gap between S_1 and T_1 state ($\Delta E_{S1\text{-}T1}$) [33]. The S_1 and T_1 ISC plays a significant role in phosphorescent process. The ISC rate decreases exponentially as $\Delta E_{S1\text{-}T1}$ increases. The minimum $\Delta E_{S1\text{-}T1}$ will enhance ISC rate and transition moment which could increase K_r. Table 6 shows that complex 5 has the largest E_{T1} (1.581 eV), the smallest value of $\Delta E_{S1\text{-}T1}$ (1.174 eV), and largest μ_{S1} (6.3D) among the complexes, which may make it has a larger emission quantum yield (Φ) than other complexes. So the designed complex 5 is possible to be good candidate for phosphorescent materials among the studied complexes.

Table 6. *The computed emitting energy (E_{T1}/eV) and the E gap between S_1 and T_1 states ($\Delta E_{S1\text{-}T1}$/eV) together with the transition electric dipole moment in the S_0 to S_1 transition (μ_{S1}/Debye).*

Complex	E_{T1}	$\Delta E_{S1\text{-}T1}$	μ_{S1}
1	1.3603	1.445	0.506
2	1.142	1.60	0.729
3	0.836	1.362	1.407
4	1.4271	1.449	1.001
5	1.5815	1.174	6.3

4. Conclusion

In this study, the five Re(I) tricarbonyl complexes containing 2, 2'- bipyridine ligand with different substituted groups (-H, $-NO_2$, $-PhNO_2$, NH_2 and -TPA) have been investigated by DFT/TDDFT methods. Specifically, the S_0 and T_1 state geometries, FMOs, absorption and phosphorescence spectra, solvent effect on absorption and emission spectra, electronic affinity, ionization potential, reorganization energy and emission quantum yield of all complexes were studied. The calculated results suggest that, the introductions of different groups on the R position of 2, 2'-bipyridine ligand have significant effect on the electronic structures and photophysical properties such as absorption and emission spectra, charge injection and transfer abilities and emission quantum yield. On the basis of FMOs analysis, for complexes 1 - 5, HOMOs energy levels have small changes, but LUMOs energy levels reveal obvious variation. Specifically, introductions of EWGs ($-NO_2$ and $-PhNO_2$) can decrease the energy level of LUMO resulting in narrower energy gap, which lead to red shifted of the lowest energy absorption bands in comparison with that of complex 1. On the contrary, introductions of EDG ($-NH_2$ and -TPA) can make the energy level of LUMO increasing, which cause the corresponding blue-shifted. The solvent effect on absorption and emission spectra indicates that lowest-energy absorption and emission bands have red-shift with the decrease of solvent polarity for these complexes. From EA, IP and λ results, we also can conclude that these complexes can be used as electron transporting materials. Moreover, the difference between $\lambda_{electron}$ and λ_{hole} of complex 5 is the smallest among these complexes, enhancing the device performance of OLEDs further. The emission quantum yield of complex 5 is possibly higher than other complexes. Therefore, complex 5 is more suitable to be used as an emitter in the PHOLEDs. Lastly, theoretical investigations can provide constructive information in the design and synthesis of novel and high-efficiency OLEDs materials. The Re(I) tricarbonyl complexes with incorporated hole transporting group to the 2, 2'-bipyridine ligand exhibit wonderful luminescent properties.

Acknowledgements

The authors acknowledge the support of the Department of chemistry, college of natural and computational science, Wollega University. Also, we acknowledge the financial support from Ministry of Science and Higher Education-Ethiopia. We also appreciate Teshome Abute, Tolesa Tesfaye, Gemechu Lemessa, Mengistu Woldetinsay, Shibiru Eticha and Chara Fedasa for their support.

Competing Interests

Authors have declared that no competing interests exist.

References

[1] Yang, R., Li, D., Bai, Y., Zhang, L., Liu, Z., Hao, J., Wei, Q., Liao, L., Peng, R. & Ge, Z. (2018). Novel tetraarylsilane-based hosts for blue phosphorescent organic light-emitting diodes. *Organic Electronics, 55,* 117-125.

[2] Naturalium, R. (n.d). Spectroscopy and photochemistry of transition metal complexes: a quantum chemical study. Dalton transactions, *39*, 9505-9513.

[3] Jia, B., Lian, H., Chen, Z., Chen, Y., Huang, J.& Dong, Q. (2017). Novel carbazole/indole/thiazole-based host materials with high thermal stability for efficient phosphorescent organic light-emitting diodes. *Journal of Dyes and Pigments, 147,* 552-559.

[4] Li, X., Zhang, D., Lu, G., Xiao, G., Chi, H., Dong, Y., Zhang, Z. & Hu, Z. (2012). Synthesis and characterization of novel rhenium (I) complexes with large Stokes shift for applications in organic electroluminescent devices. *Journal of Photochemistry and Photobiology A: Chemistry*, *241*, 1-7.

[5] Chung, W.-K., Maggie, Ng., Zhu, N., Siu, S. K.-L. & Yam, V. W.-W. (2017). Synthesis, characterization and computational studies of luminescent rhenium(I) tricarbonyl diimine complexes with 8-hydroxyquinoline containing alkynyl ligands. *Journal of Organometallic Chemistry*. DOI: 10.1021/acs.inorgchem.6b02999.

[6] Nahhas, A. E., Consani, C., Blanco, A. M, Lancaster, K. M., Braem, O., Cannizzo, A., Towrie, M., Clark, I., Zalis, S., Chergui, M. & Vlcek, A. (2011). Ultrafast ExcitedState dynamics Re(I) Photosensitizers $[Re(Cl)(CO)_3(N,N)]$ & $[Re(imidazole)(CO)_3(N,N)]^{n+}$: Diimine Effects. *American chemical society, 50,* 2932-2943.

[7] Huang, T. T. & Li, E. Y. (2016). Enhanced spin-orbit coupling driven by state mixing in organic molecules for OLED applications. *Organic Electronics, 39,* 311-317.

[8] Maisuls, I., Wolcan, E., Piro, O. E., Castellano, E. E., Petroselli, G., Erra-Balsells, R., Cabrerizo, F. M. & Ruiz, G. T. (2017). Synthesis, Structural Characterization and Biological Evaluation of Rhenium (I) Tricarbonyl Complexes with -Carboline Ligands. *Inorganic chemistry*, *2*, 8666-8672.

[9] Bertrand, H. C., Clede, S., Guillot, R., Lambert, F. & Policar, C. (2014). Luminescence Modulations of Rhenium Tricarbonyl Complexes Induced by Structural Variations. *Inorganic chemistry*.dx.doi.org/10.1021/ic5007007.

[10] Rohman, M. A., Sutradhar, D., Sangilipandi, S., Rao, K. M., Chandra, A. & Mitra, S. (2017). Photophysical behavior of systematically substituted (di-2-pyridylaminomethyl) benzene ligands and its Re(I) complexes: A combined experimental and theoretical approach. *Journal of Photochemistry and Photobiology A: Chemistry*. http://dx.doi.org/10.1016/j.jphotochem.2017.03.031.

[11] Liu, S., Li, Y., Hu, X., Liu, X. & Guan, B. (2017). DFT studies on the ligand effect on electronic and optical properties of three series of functionalized Ir(III) complexes. *Journal of Molecular Structure*, *1151*, 49-55.

[12] Ramos, L. D., Cruz, H. M. D. & Frin, K. P. M. (2017). Photophysical properties of Rhenium(I) complexes and photo-sensitized generation of singlet O_2. *Photochemical & Photobiological Sciences*, *16*, 459-466.

[13] Shillito, G. E., Hall, T. B. J., Preston, D., Traber, P., Wu, L., Reynolds, K. E. A., Horvath, R., Sun, X. Z., Lucas, N. T., Crowley, J. D., George, M. W., Kupfer, S. & Gordon, K. C. (2018). Dramatic Alteration of ^{3}ILCT Lifetimes Using Ancillary Ligands in $[Re(L)(CO)_3(phen\text{-}TPA)]^{n+}$ Complexes: An Integrated Spectroscopic and Theoretical Study. *Journal of the American Chemical Society*, *140*, 4534-4542.

[14] Garino, C. & Salassa, L. (2013). The photochemistry of transition metal complexes by density functional theory. Philosophical Transactions of Royal Society A. http://dx.doi.org/10.1098/rsta.2012.0134.

[15] Wang, J.-X., Xia, H.-Y., Liu, W.-Q., Zhao, F.& Wang, Y.-b. (2012). Synthesis, spectroscopic and DFT studies of rhenium (I) complexes with phenanthrolineimidazo ligands containing thienyl moieties. *Inorganica Chimica Acta, 394,* 92-97.

[16] Velmurugan, G., Ramamoorthi, B.& Venuvanalingam, P. (2014). Are Re(I) phenanthroline complexes suitable candidates for OLEDs? Answers from DFT and TD-DFT investigations. *Royal society of chemistry*. DOI: 10.1039/c4cp01135j.

[17] Wang, M., Liu, G.-B., Guo, H. & Yao, Y. (2017). An efficient method for hybrid density functional calculation with spin-orbit coupling. *Computer Physics Communications*. https://doi.org/10.1016/j.cpc.2017.11.010.

[18] Plascencia, C., Wan, J.& Wilson, A. K., (2017). Importance of the ligand basis set in ab initio thermochemical calculations of transition metal species. *Chemical Physics Letters*. DOI*:* http://dx.doi.org/10.1016/j.cplett.2017.08.003.

[19] Ermler, C. W. & Tilson, J. L. (2012). Generally contracted valence-core/valence basis sets for use with relativistic effective core potentials and spin-orbit coupling operators. *Computational and Theoretical Chemistry, 1002,* 24-30.

[20] Sangilipandi, S., Nagarajaprakash, R., Sutradhar, D., Kaminsky, W., Chandra, A. K. & Rao, K. (2015). Synthesis, molecular structural studies and DFT calculations of tricarbonyl rhenium(I) metal complexes containing nitrogen based N^N donor polypyridyl ligands. *Inorganica Chimica Acta*, *437*, 177-187.

[21] Yang, X.-Z., Wang, Y.-L., Guo, J.-Y, Zhang, T.-T., Jia, J.-F. & Wu, H.-S. (2016). The effect of group-substitution on structures and photophysical properties of rhenium(I) tricarbonyl complexes with pyridyltetrazole ligand: A DFT/TDDFT study. *Journal of Materials Chemistry and Physics, 178,* 173-181.

[22] Zhao, F., Wang, J-x.& Wang, Y-b. (2011). DFT/TDDFT theoretical studies on electronic structures and spectral properties of rhenium(I) phenanthrolineimidazo complexes. *Computational and Theoretical Chemistry*, *985*, 90-96.

[23] Zhao, F., Wang, J., Liu, W.-q.& Wang, Y. (2012). Electronic structures and spectral properties of rhenium(I) tricarbonyl diimine complexes with phosphine ligands: DFT/TDDFT theoretical investigations. *Computational and Theoretical Chemistry, 973,* 40-46.

[24] Vincendon, M., Lacombe, L., Dinh, P. M., Suraud, E. & Reinhard, P. G. (2017). Time dependent DFT in natural orbitals. *Computational Materials Science, 138,* 426-434.

[25] Ullrich, C. A. & Yang, Z.-H. (2014). A brief compendium of time-dependent density-functional theory. Columbia, USA, *2*, 1305-1388.

[26] Tyminska, N. (2013). Modern Computational Chemistry Methods for Prediction of Ground and Excited-State Properties in Open Shell Systems. Dissertations, Master's Thesis & Master's Reports.

[27] Han, D., Liu, J., Miao, R., Zhao, L. & Zhang, G., (2014). Theoretical design study on the electronic structure and photophysical properties of a series of osmium(II) complexes with different ancillary ligands. *Polyhedron, 85,* 506-510.

[28] Xia, H., Zhao, F., Liu, W.& Wang, Y. (2012). Electronic structures and spectral properties of rhenium (I) tricarbonyl cyclopenta[b]dipyridine complexes containing different aromatic ring groups. *Journal of Organometallic Chemistry, 727,* 10-18.

[29] Świtlicka-Olszewska, A., Klemens, T., Nawrota, I., Machura, B. & Kruszynski, R. (2015). Novel Re(I) tricarbonyl coordination compound of 5-amino-1,10-phenanthroline-Synthesis, structural, photophysical and computational studies. *Journal of Luminescence, 171,* 166-175.

[30] Zhang, T.-T., Jia, J.-F., Ren, Y.& Wu, H.-S. (2011). Ligand Effects on Structures and Spectroscopic Properties of Pyridine-2-aldoxime Complexes of $Re(CO)_3$ Theoretical Studies. *Journal of physical chemistry, 115*, 3174-3181.

[31] Seminario, J. M. (2007). Molecular and Nano Electronics: Analysis, Design and Simulation. Texas, USA, *17*, 24-27.

[32] Baryshnikov, G., Minaev, B. & Agren, H. (2017). Theory and Calculation of the Phosphorescence Phenomenon. *Chemical Reviews*, *117*, 6500-6537.

[33] Gouralouen, C., Eng, J., Otsuka, M., Gindensperger, E.& Daniel, C. (2014). A Quantum Chemical Interpretation of Ultrafast Luminescence Decay and Intersystem Crossings in Rhenium(I) Carbonyl Bipyridine Complexes. *Journal of Chemical Theory and Computation*. DOI: 10.1021/ct500846n.

[34] Kia, R.& Safari, F. (2016). Synthesis, spectral and structural characterization and computational studies of rhenium(I)-tricarbonyl nitrito complexes of 2, 2′-bipyridine and 2,9-dimethylphenanthroline ligands: π-accepting character of the diimine ligands. *Inorganica Chimica Acta*. DOI: http://dx.doi.org/10.1016/j.ica.2016.08.041.